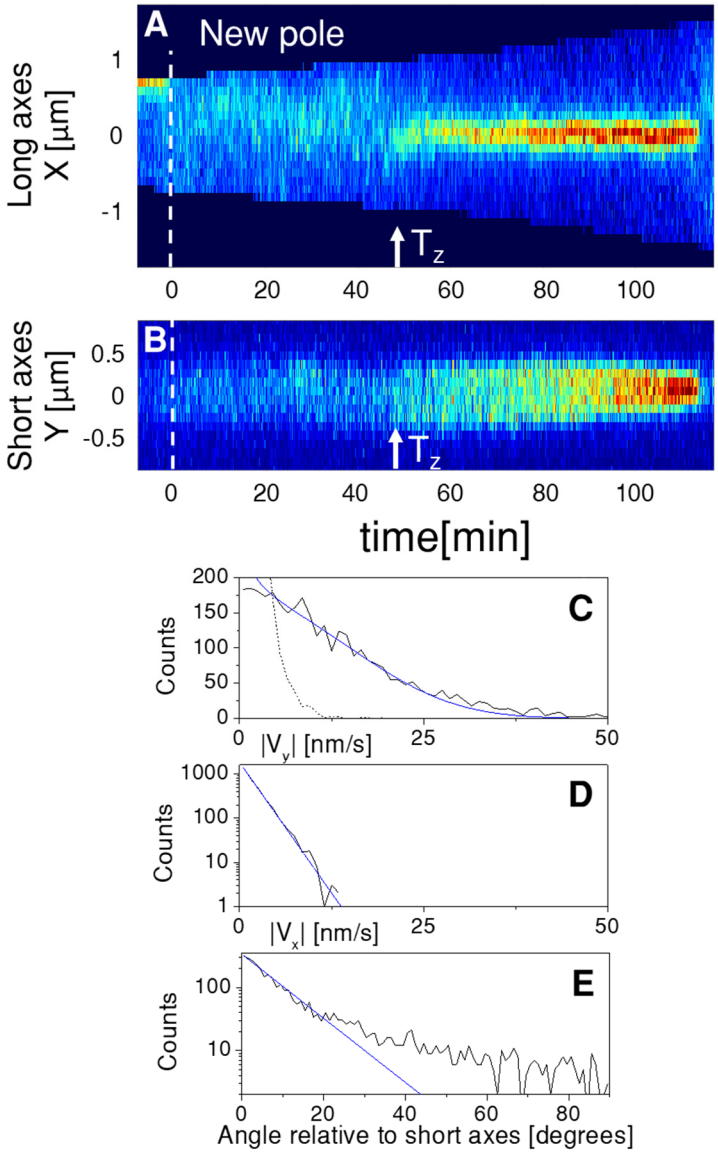

Figure S1. **Data from a representative cell expressing FtsZ C-terminal fusion to GFP from a plasmid (strain JM60), Related to Figure 1.**

(A, B) Kymographs of FtsZ-GFP intensity distribution along the long axis (A) and short axis (B) of the cell. Red corresponds to high concentrations while blue corresponds to low concentrations. Vertical dashed lines correspond to times of cell birth and white arrow corresponds to Z-ring formation time (T_z). (C) Distribution of apparent speeds of assemblies relative to the short axis of the cell (black). Blue line is a fitting of the distribution taking into account the variation of the apparent speeds on the cell perimeter (Methods: *Distribution of Apparent Treadmilling Speeds*). The fitting yields true speeds of 15±11 nm/s (mean±std). (D) Distribution of apparent speeds of FtsZ assemblies relative to the long axis of the cell (black). Blue line is exponential fitting of the distribution. The decay constant from the fitting is 1.8 nm/s. (G) Angles of velocity vectors relative to the short axis of the cell (black). Blue line is exponential fitting of angles 0-20°. The characteristic angle from the fitting is 9.2°. In panels (E-F) the number of cells analyzed is N_{cell}=18 and number of transient assemblies analyzed $N_{cluster}$= 408.

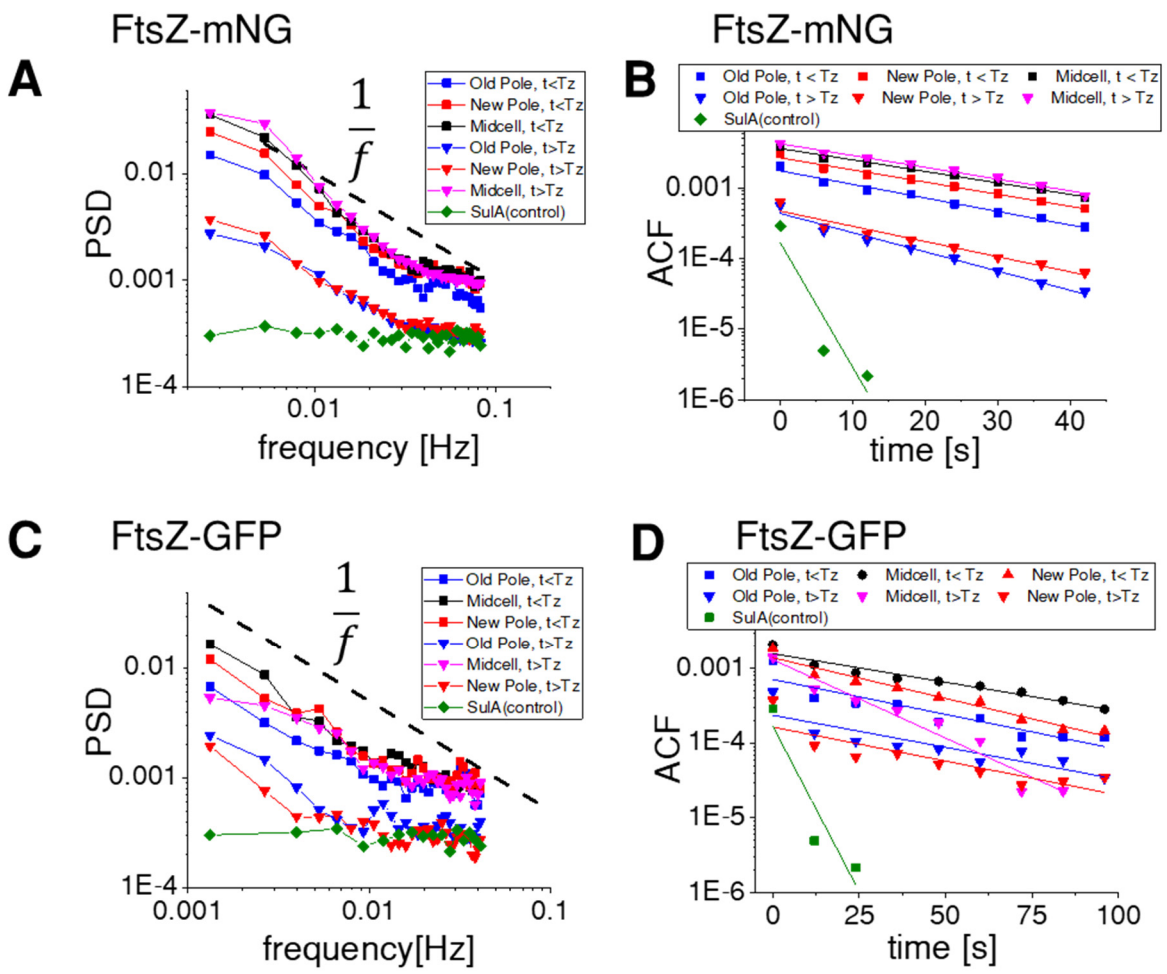

Figure S2. Comparison of FtsZ-mNG (JM26) to FtsZ-GFP (JM60) fluctuations before and after Z-ring formation, Related to Figure 2.

(A, B) Population averaged (N = 20) power spectral density before (squares) and after (triangles) Z-ring formation in JM26 strain expressing endogenously FtsZ-mNG. In addition to traces from cell quarter positions, midcell data are shown. Dashed black line shows for reference an inverse frequency dependence. Control data (diamonds) is from cells where FtsZ polymerization is inhibited by upregulation of SulA (N=10). (B) Population averaged (N = 20) autocorrelation function before and after T_z. Exponential fits to the autocorrelation functions are shown by solid lines and experimental data by markers. (C) Population averaged (N=18) power spectral density analysis of strain expressing FtsZ-GFP from a plasmid (strain JM60) before and after T_z. (D) Population averaged (N=18) autocorrelation function for this strain before and after T_z. Exponential fits to the autocorrelation functions are shown by solid lines and experimental data by markers.

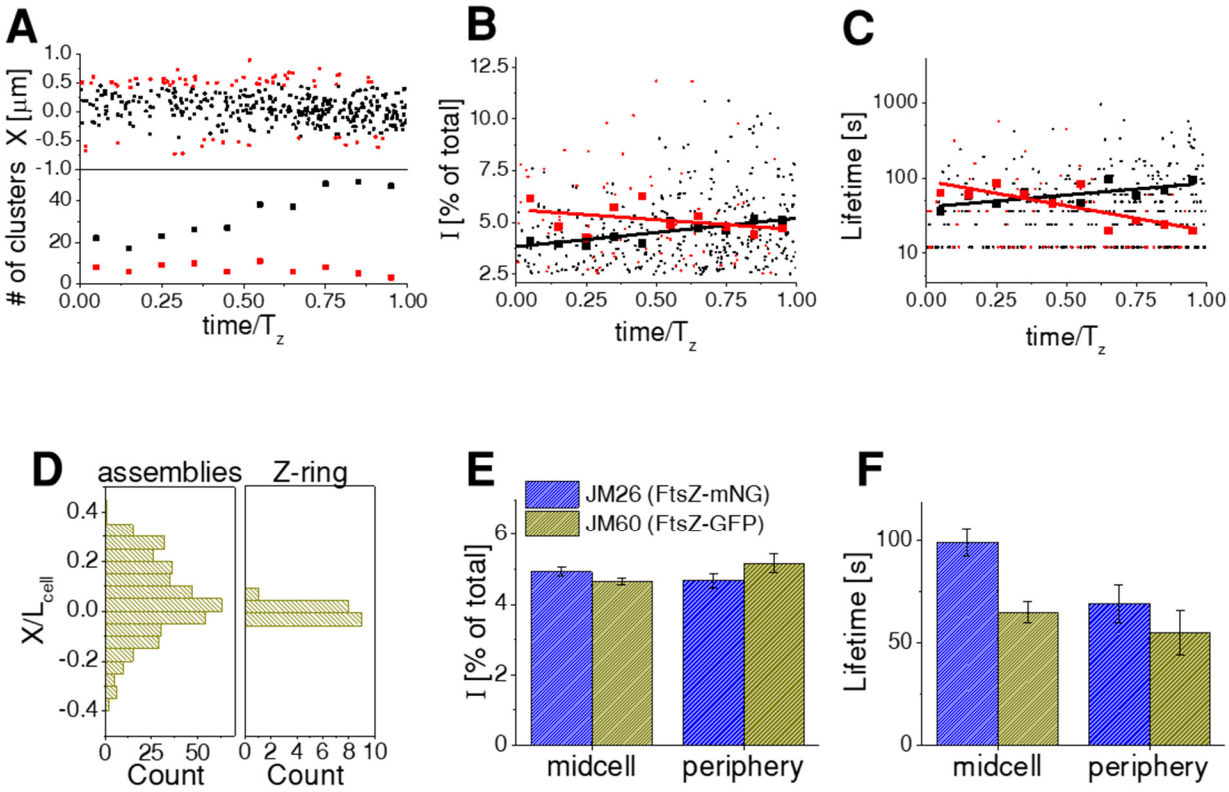

Figure S3. Characterization of spatial and temporal distribution of FtsZ transient assemblies in JM60 strain where FtsZ-GFP is expressed from a plasmid, Related to Figure 3.

Only assemblies that contain 2.5% or higher amounts of FtsZ relative to the cell total are shown. Solid lines in different panels are linear fits. Numbers on the top of the panel indicate average values. Parameters of fits, numbers of cells, and clusters analyzed are collected to Table S2. (A) Top: The positions of assemblies along the long axis of the cell as a function of time. Assemblies at midcell are shown by black and in cell peripheries by red markers. Time axis is scaled by time when the Z-ring forms (T_z). Bottom: Number of assemblies in midcell and two peripheries combined as a function of normalized time. Solid lines in panels (A)-(C) are linear fits. (B) The fluorescent intensities from assemblies as function of normalized time. The intensities are scaled by the total fluorescent intensity from the cell and averaged over the lifetime of each assembly. The small markers are individual data points and the large markers the binned data. (C) Lifetimes of assemblies at the midcell (black) and in the periphery (red) as a function of normalized time. (D) Distribution of assemblies (left) and Z-ring positions (right) along the long axes of the cell. Positions are normalized by the cell length. Panels (A)-(D) correspond to FtsZ-GFP cells (strain JM60). (E) Comparison of sizes of assemblies in FtsZ-mNG (JM26) and FtsZ-GFP (JM60) strains. (F) Comparison of lifetimes of the assemblies in these two strains. In the last two panels error bars are std error.

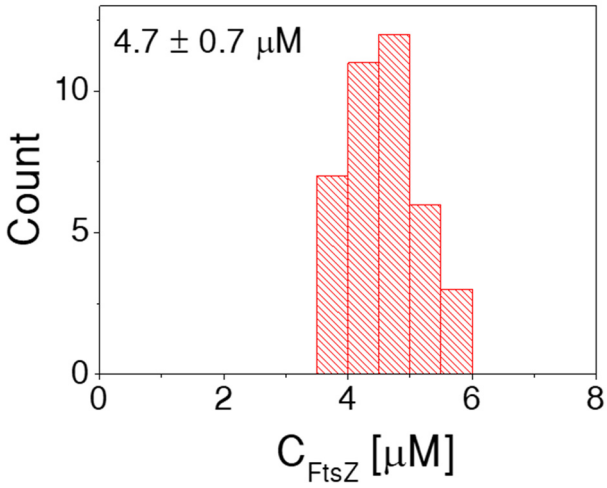

Figure S4. Determination of FtsZ concentration in *E. coli* cells growing in M9 glycerol medium (strain KC606), Related to Figure 4.

In this determination fluorescent intensity from cells were compared to the fluorescent intensity from a GFP standard as explained in more details in Methods: *Determination of total FtsZ numbers in cells*. In the measurements 42 channels were used. Of those, 21 were 0.8 μm wide and the remaining half were 0.9 μm wide. The channels were first filled with GFP and then populated with cells. The average concentration of 4.7±0.7 μM (mean±std) was determined.

Strain	Genotype	Antibiotics used: plates/ liquid culture
JM26	BW27783 ftsZ::ftsZ$^{55\text{-}56}$-mNeonGreen ΔmotA:: frt-Kan-frt	25 μg/ml Kan
JM60	BW27783 ColEI, PT5-lac::6xHis-ftsZ-GFP, Cm^{R}	40 μg/ml Cm (plates; PDMS chip) 80 μg/ml Cm (liquid)
KC606	BW25113 ftsZ::ftsZ$^{55\text{-}56}$-sfGFP	
BEW1	BW27783 ftsZ::ftsZ$^{55\text{-}56}$-mNeonGreen ΔminC:: frt-Kan-frt	25 μg/ml Kan
BEW2	BW27783 ftsZ::ftsZ$^{55\text{-}56}$-mNeonGreen ΔzapA:: frt-Kan-frt	25 μg/ml Kan
MB43	BW27783 ftsZ::ftsZ$^{55\text{-}56}$-mNeonGreen P_{lac}sulA, Cm^{R}	30 μg/ml Cm 0.2% glucose, except during induction
JM71	MG1655 lacY::lacY-mNeonGreen-frt-Kan-frt	25 μg/ml Kan
HE5	JKD7 ftsZ:: Kan pJSB -ftsZ$^{55\text{-}56}$-mMaple3; Cm^{R}	30 μg/ml Cm 25 μg/ml Kan
JM95	BW25113 ftsZ::ftsZ$^{55\text{-}56}$-sfGFP-CM ΔzapA::frt-kan-frt	25 μg/ml Cm 30 μg/ml Kan

Table S1. List of the strains used in experiments. Related to STAR Methods.

JM26 was constructed by P1 transduction of the ΔmotA743::kan allele from Keio collection [S1] strain JW1879-2 into BW27783 ftsZ::ftsZ$^{55\text{-}56}$-mNeonGreen [S2] (a gift from Dr. H. Erickson).

JM60 was created by transformation of BW27783 strain with plasmid JW0093 (ColEI, PT5-lac::6xHis-ftsZ-gfp cm [S3]) (gift from Dr. J. Xiao)

KC606 strain received from Dr. J. Xiao Lab [S3].

BEW1 was constructed by P1 transduction of the ΔminC765::kan allele from Keio collection strain JW1165 into BW27783 ftsZ::ftsZ$^{55\text{-}56}$-mNeonGreen.

BEW2 constructed by P1 transduction of the ΔzapAA761::kan allele from Keio collection strain JW2878-1 into BW27783 ftsZ::ftsZ$^{55\text{-}56}$-mNeonGreen.

MB43 was created by transformation of BW27783 ftsZ::ftsZ$^{55\text{-}56}$-NeonGreen strain with pA3 plasmid containing *sulA* sequence [S4] (gift from Dr. A. Dajkovic).

JM71 was constructed by λ-Red engineering [S5] of the C-terminal fusion of mNeonGreen to LacY using the strain MG1655. First, the mNeonGreen (mNG) gene sequence was amplified from the strain JM26 and cloned into pROD62 plasmid (a gift from Dr. R. Reyes-Lamothe) using Gibson assembly protocol according to manufacturer's instructions (New England BioLabs Inc). The resulting template plasmid carries a copy of mNG followed by kanamycin resistance cassette flanked by *frt* sites and a flexible linker peptide SAGSAAGSGEF between mNG and the protein targeted. Primers carrying 40nt tails with identical sequence to the chromosomal locus for insertion were used to amplify the linker -mNG-*frt*-kan^{R}-*frt* from template plasmid. The resulting PCR product was transformed by electroporation into a strain carrying the λ-Red -expressing plasmid pKD46. Colonies were selected by kanamycin resistance and fluorescence microscopy.

HE5 strain received from Dr. H. Erickson lab. Described in [S2].

JM95 KC606 were transduced with P1 viral lysate of ZapA deletion strain from Keio collection JW2878-1. This strain is CM^{R} at 25 and Kan^{R} at 30 ug/ml.

		Figures 3B and S3B		Figures 3C and S3C	
Strain	**Location**	**Slope**	**Pearson R**	**Slope**	**Pearson R**
JM26 (mNG) (N_{cell} = 20)	Midcell (N_{clust} = 257)	0.97 ± 0.41	0.14	75 ± 48	0.09
JM26 (mNG) (N_{cell} = 20)	Periphery (N_{clust} = 81)	-0.01 ± 0.67	-0.001	13 ± 29	0.05
JM60 (GFP) (N_{cell} = 18)	Midcell (N_{clust} = 336)	1.37 ± 0.34	0.22	46 ± 17	0.69
JM60 (GFP) (N_{cell} = 18)	Periphery (N_{clust} = 72)	-0.95 ± 0.74	-0.42	-62 ± 20	-0.74

Table S2. Parameters of linear fits in Figures 3 and S3. Related to Figure 3 and S3.

N_{cell} corresponds to the number of cells analyzed and N_{clust} to the total numbers of transient assemblies analyzed.

Supplemental References

S1. Baba, T., Ara, T., Hasegawa, M., Takai, Y., Okumura, Y., Baba, M., Datsenko, K.A., Tomita, M., Wanner, B.L., and Mori, H. (2006). Construction of *Escherichia coli* K-12 in-frame, single-gene knockout mutants: the Keio collection. Mol. Syst. Biol. *2*, 1-11.

S2. Moore, D.A., Whatley, Z.N., Joshi, C.P., Osawa, M., and Erickson, H.P. (2017). Probing for binding regions of the FtsZ protein surface through site-directed insertions: discovery of fully functional FtsZ-fluorescent proteins. J. Bacteriol. *199*, 17.

S3. Yang, X.X., Lyu, Z.X., Miguel, A., McQuillen, R., Huang, K.C., and Xiao, J. (2017). GTPase activity-coupled treadmilling of the bacterial tubulin FtsZ organizes septal cell wall synthesis. Science *355*, 744.

S4. Dajkovic, A., Mukherjee, A., and Lutkenhaus, J. (2008). Investigation of regulation of FtsZ assembly by SulA and development of a model for FtsZ polymerization. J. Bacteriol. *190*, 2513-2526.

S5. Datsenko, K.A., and Wanner, B.L. (2000). One-step inactivation of chromosomal genes in Escherichia coli K-12 using PCR products. Proc. Natl. Acad. Sci. U. S. A. *97*, 6640-6645.